

## Isobaric-Analog Resonances in Se Isotopes\*

D. P. BALAMUTH,<sup>†</sup> G. P. COUCHELL, AND G. E. MITCHELL  
*Columbia University, New York, New York 10027*

(Received 8 February 1968)

Isobaric-analog resonances have been observed by measuring excitation curves for  $(p,p)$  elastic scattering from  $^{76}\text{Se}$ ,  $^{78}\text{Se}$ ,  $^{80}\text{Se}$ , and  $^{82}\text{Se}$ . Excitation curves were also measured for the  $(p,n)$  reaction on  $^{78}\text{Se}$ ,  $^{80}\text{Se}$ , and  $^{82}\text{Se}$ . All resonances observed in elastic scattering have been fitted using a Coulomb-plus-single-level formula, and  $l$  values and resonance parameters have been extracted. The level positions and  $l$  values agree quite well with a recent  $(d,p)$  study of the selenium isotopes, except for one case where two isobaric-analog resonances were reported as a single state in the  $(d,p)$  work. Coulomb energy differences have been computed for the four pairs of nuclei ( $^{77}\text{Se}$ ,  $^{77}\text{Br}$ ), ( $^{79}\text{Se}$ ,  $^{79}\text{Br}$ ), ( $^{81}\text{Se}$ ,  $^{81}\text{Br}$ ), and ( $^{83}\text{Se}$ ,  $^{83}\text{Br}$ ). Spectroscopic factors have also been calculated for all resonances observed in elastic scattering; these are compared with the spectroscopic factors extracted from the stripping data.

### 1. INTRODUCTION

ISOBARIC-ANALOG resonances<sup>1,2</sup> in the compound nucleus have been observed in many nuclei since their discovery by Fox, Moore, and Robson<sup>3</sup> in 1964. Good agreement has generally been found<sup>4</sup> between the analog resonances and the levels of the residual nucleus observed in  $(d,p)$  reactions on the same target.

In the present work<sup>5</sup> excitation curves for proton elastic scattering have been measured for the four even-mass selenium isotopes,  $^{76}\text{Se}$ ,  $^{78}\text{Se}$ ,  $^{80}\text{Se}$ , and  $^{82}\text{Se}$ , which are available in high enrichments. Excitation curves for the  $(p,n)$  reaction have also been measured for these isotopes, with the exception of  $^{76}\text{Se}$ , which has the neutron channel closed in the energy region of interest. The selenium isotopes are of interest for two reasons. First, it is possible to study the behavior of isobaric-analog resonances as a function of neutron excess. Second, the availability of a recent  $(d,p)$  study<sup>6</sup> of all four isotopes makes possible detailed comparison between level positions and spectroscopic properties observed in the  $(d,p)$  study and in the present work.

All  $(p,n)$  and  $(p,p)$  excitation curves displayed resonances which are identified as the isobaric analogs of states in the adjacent odd-mass selenium isotopes  $^{77}\text{Se}$ ,  $^{79}\text{Se}$ ,  $^{81}\text{Se}$ , and  $^{83}\text{Se}$ . The resonances in the elastic scattering excitation curves were fitted assuming the cross section to be Rutherford scattering plus the contributions from a number of "single levels." (The "single levels" observed in this poor-resolution (5–10 keV) experiment are of course the result of averaging over the fine structure of the analog state.) The resonance parameters which gave the best fit to the experimental

data have been extracted. The over-all agreement between the present  $(p,n)$  and  $(p,p)$  work is very good. All resonances which were observed with elastic scattering also occurred in the  $(p,n)$  excitation curves; however, a number of resonances observed in the  $(p,n)$  reaction were not seen in elastic scattering.

In this paper the target will be denoted by  $C$ . The proton-plus-target (compound nucleus) system will be called  $pC$ , and the neutron-plus-target (parent) system will be called  $nC$ . The theory of isobaric-analog resonances<sup>1</sup> predicts that the elastic-proton reduced widths of the resonances in the  $pC$  system should be related to the neutron reduced widths of the levels in the parent nucleus  $nC$  by

$$\gamma_p^2 = \gamma_n^2 / (2T_0 + 1), \quad (1.1)$$

where  $T_0$  is the isospin of the target. Spectroscopic factors, which are essentially equivalent to reduced widths  $\gamma_p^2$ , have been calculated for all isobaric-analog resonances observed with elastic scattering. These spectroscopic factors are compared with spectroscopic factors obtained from the  $(d,p)$  stripping data of Lin.<sup>6</sup>

### 2. EXPERIMENTAL PROCEDURE AND DATA REDUCTION

The proton beam was obtained from the Columbia University 5.5-MeV Van de Graaff accelerator. Scattered protons were detected by three silicon surface-barrier detectors, which were placed at angles of  $90^\circ$ ,  $125^\circ$ , and  $150^\circ$  with respect to the incident beam. These angles correspond approximately to the zeros of the Legendre polynomials  $P_{\text{odd}}$ ,  $P_2$ , and  $P_4$ . The  $l$  value of a resonance is inferred from lack of resonant structure at the angle corresponding to the zero of the  $l$ th Legendre polynomial. In addition to the usual energy calibration using the  $^7\text{Li}(p,n)^7\text{Be}$  threshold, the known resonance<sup>7</sup> in  $^{12}\text{C}(p,p)^{12}\text{C}$  at 4.806 MeV was used as a secondary calibration.

The targets for this experiment were prepared by evaporating isotopically enriched selenium (86.1%  $^{76}\text{Se}$ , 96.0%  $^{78}\text{Se}$ , 97.8%  $^{80}\text{Se}$ , 89.1%  $^{82}\text{Se}$ ) onto backings of

\* Work partially supported by the U. S. Atomic Energy Commission.

<sup>†</sup> National Science Foundation Predoctoral Fellow.

<sup>1</sup> D. Robson, Phys. Rev. **137**, B535 (1965).

<sup>2</sup> C. Mahaux and H. A. Weidenmüller, Nucl. Phys. **89**, 33 (1966).

<sup>3</sup> J. D. Fox, C. F. Moore, and D. Robson, Phys. Rev. Letters **12**, 198 (1964).

<sup>4</sup> *Isobaric Spin in Nuclear Physics*, edited by J. D. Fox and D. Robson (Academic Press Inc., New York, 1966).

<sup>5</sup> A preliminary version of part of this work was presented at a recent American Physical Society meeting: D. P. Balamuth, G. P. Couchell, and G. E. Mitchell, Bull. Am. Phys. Soc. **12**, 1042 (1967).

<sup>6</sup> E. K. Lin, Phys. Rev. **139**, B340 (1965).

<sup>7</sup> C. W. Reich, G. C. Phillips, and J. L. Russell, Jr., Phys. Rev. **104**, 143 (1956).

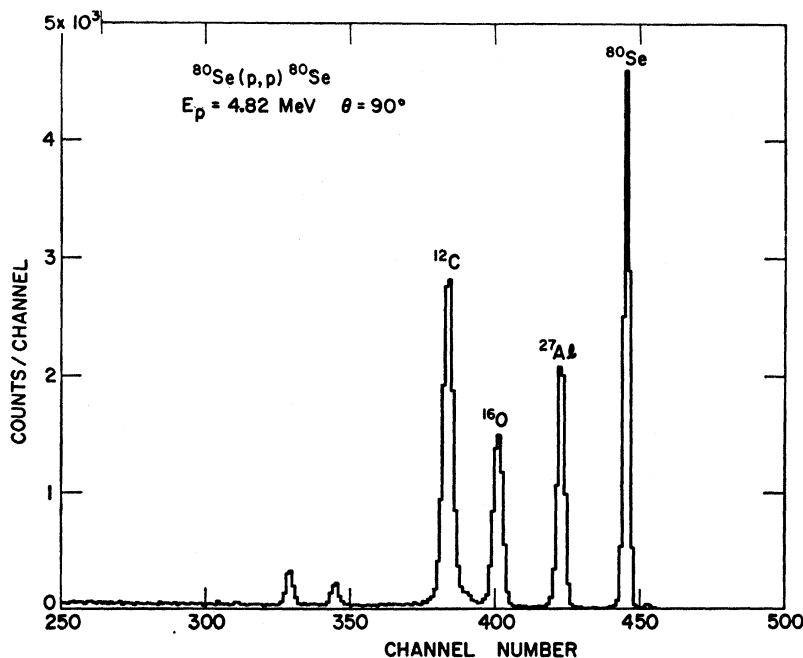


FIG. 1. Typical spectrum. The presence of aluminum is explained in the text.

Formvar coated with a thin layer of aluminum. The aluminum was used to dissipate the heat generated by the proton beam. Targets of selenium without the conducting layer of aluminum deteriorated under a beam of  $\sim 0.01 \mu\text{A}$ ; with the aluminum layer, beams of  $\sim 0.025 \mu\text{A}$  did not damage the targets. The targets were approximately  $75 \mu\text{g}/\text{cm}^2$ , which corresponds to an energy loss of about 3 keV for 5-MeV protons.

The signals from the charged-particle detectors were amplified and sent to an RCL 512-channel pulse-height analyzer. A typical spectrum is shown in Fig. 1. The over-all experimental energy resolution was about 35 keV. Under actual running conditions, the spectrum from each angle was stored in 128 channels; the proton elastic scattering peaks from  $^{12}\text{C}$  and  $^{16}\text{O}$  were biased out, in order to reduce dead-time losses.

The spectra were dumped from the analyzer directly into a PDP-4 computer. The areas of the selenium elastic scattering peaks were calculated by the computer, after a suitable background subtraction. While one set of data was processed by the computer, the next data point was collected in the multichannel analyzer. Each point took 5–8 min to accumulate; the data processing was easily accomplished in this time. Typically,  $5 \mu\text{C}$  of charge were collected for each point.

At energies of about 5 MeV,  $\alpha$  particles from the  $^{27}\text{Al}(p,\alpha)^{24}\text{Mg}$  reaction have the same energy as protons elastically scattered from selenium at  $150^\circ$ . Since the  $^{27}\text{Al}(p,\alpha)^{24}\text{Mg}$  reaction goes through a number of strong resonances in this energy region, a separate excitation curve was measured for this reaction using a thin aluminum target. After normalizing the excitation curves, using the elastic proton scattering peak from aluminum, a subtraction was made of the  $^{27}\text{Al}(p,\alpha)^{24}\text{Mg}$  contribution at  $150^\circ$ .

The experimental arrangement for measuring the  $(p,n)$  yield has been described previously.<sup>8</sup> Neutrons were detected at  $90^\circ$  with a  $^3\text{He}$ -filled proportional counter embedded in paraffin. Targets were prepared by evaporating selenium onto 0.005-in. tantalum backings. Target thicknesses were approximately  $100 \mu\text{g}/\text{cm}^2$ .

### 3. ANALYSIS OF RESONANCE PARAMETERS AND RESULTS

#### General

The analysis of the  $(p,p)$  excitation curves to extract the resonance parameters was done using the computer program SNOW,<sup>9</sup> written by Moore and Richard. This program performs a nonlinear least-squares fit<sup>7</sup> of the data to the following expression:

$$\frac{d\sigma}{d\sigma}(E,\theta) = \frac{\pi}{2k^2} \sum_{mm'} \left| c(E,\theta) \delta_{mm'} + \sum_{\lambda} (2l_{\lambda} + 1)^{1/2} C(\frac{1}{2}l_{\lambda} J_{\lambda}; m 0 m) \times C(\frac{1}{2}l_{\lambda} J_{\lambda}; m', m - m', m) \times \frac{e^{2i\omega_{l\lambda}} \Gamma_{\lambda p}}{E_{\lambda} - E - \frac{1}{2}i\Gamma_{\lambda}} Y_{l_{\lambda}}^{m-m'}(\theta, \phi) \right|^2, \quad (3.1)$$

where  $c(E,\theta) = (1/2\sqrt{\pi})\eta \csc^2(\frac{1}{2}\theta) e^{-2i\gamma}$ ,

$$\gamma = \eta \ln \sin \frac{1}{2}\theta,$$

$$\eta = 0.15748 (M/E)^{1/2},$$

$$\omega_l = \sum_{m=1}^l \tan^{-1} \left( \frac{\eta}{m} \right).$$

<sup>8</sup> G. P. Couchell, D. P. Balamuth, R. N. Horoshko, and G. E. Mitchell, Phys. Rev. **161**, 1147 (1967).

<sup>9</sup> C. F. Moore and P. Richard, SNOW, Florida State University Technical Report No. 8, 1965 (unpublished).

TABLE I. Resonance parameters of resonances observed in  $(p,p)$  and  $(p,n)$  reactions, and comparison with  $(d,p)$  experiment by Lin (Ref. 6).

Nucleus	$(p,p)$					$(p,n)$				$(d,p)^a$	
	$E_p$ (MeV)	$E_{o.m.}$ (MeV)	$\Gamma_{tot}$ (keV)	$(2J+1)\Gamma_p$ (keV)	$l_p$	$E_p$ (MeV)	$E_{o.m.}$ (MeV)	$\Gamma_{tot}$ (keV)	$E_{ex}$ (MeV)	$E_{ex}$ (MeV)	$l_p$
$^{76}\text{Se}$	4.146 <sup>b</sup>	4.092	20± 8	4.9± 2.0	0				0.97	0.97	0
	4.272	4.216	24± 5	9.0± 2.0	0				1.09	1.15	0
$^{78}\text{Se}$	4.694	4.635	43± 5	29.4± 3.0	0	4.697	4.638	46±10	1.16	1.16	0
	4.808	4.747	24± 9	13.5± 6.0	2	4.810	4.749	38±10	1.27	1.25	2
	5.089	5.025	16± 5	3.6± 1.0	0	5.088	5.024	35±10	1.55	1.49	(0)
						5.168	5.103	35±10	1.63	1.60	2
						5.296	5.229	...	1.75	1.67	2
						5.363	5.295	...	1.82	1.76	2
$^{80}\text{Se}$	3.817	3.770	15± 5	1.9± 0.6	1	3.827 <sup>c</sup>	3.780	16± 5	0	0	1
						3.934 <sup>c</sup>	3.885	...	0.11	0.10	4
						4.302 <sup>c</sup>	4.249	...	0.47	0.47	1
	4.847	4.787	14± 5	8.8± 3.0	2	4.851	4.791	14± 5	1.02	1.06	2
	4.982	4.920	44± 5	37.6± 4.0	0	4.984	4.922	63±20	1.15	1.25	0
	5.060	4.998	35± 5	27.6± 4.0	2	5.066	5.003	34±10	1.23	1.31	2
$^{82}\text{Se}$						4.899	4.840	...	0.36	0.36	(0)
						4.977 <sup>d</sup>	4.917	...	0.44	0.43	2
	5.148	5.086	47± 5	35.2± 3.5	0	5.149	5.087	90±30	0.61	0.59	2
	5.190	5.127	42±10	43.8±12.0	2	5.187	5.124	30±10	0.65		

<sup>a</sup> From Ref. 6.<sup>b</sup> All energies are believed accurate to ±0.010 MeV.<sup>c</sup> From Ref. 8.<sup>d</sup> Possibly partly due to contaminant of  $^{80}\text{Se}$  in target.

In these equations,  $M$  is the reduced mass of the system in units of amu, and  $E$  is the center-of-mass energy in MeV. The parameters characterizing a resonance, in addition to spin and parity, are the resonance energy  $E_\lambda$ , the resonance total width  $\Gamma_\lambda$ , and the resonance partial width for proton elastic scattering,  $\Gamma_{\lambda p}$ .

This formula represents the elastic scattering of a spin- $\frac{1}{2}$  projectile by a spin-zero target. The scattering amplitude consists of a potential term  $c(E,\theta)$ , which in the present work was taken to be Rutherford scattering, plus a sum of terms representing isolated resonances of different spin and parity. The effects of nuclear potential scattering are small at energies well below the Coulomb barrier and have been neglected. Interference effects between neighboring resonances of the same spin and parity have likewise been neglected. For the isobaric analogs of low-lying, well-separated states this is a good approximation.

In practice the  $l$  value of a resonance was determined by inspection of the resonance angular distribution; the program then used this information, together with guesses for the resonance parameters, to calculate the values of  $E_\lambda$ ,  $\Gamma_\lambda$ , and  $(2J+1)\Gamma_{\lambda p}$  which gave the best fit to the data.

Resonance parameters were extracted from the  $(p,n)$  excitation curves using a graphical technique. Since the resonances were superimposed on a rising neutron background, a background curve was drawn which made a smooth connection with the excitation curve on each side of the resonance. The background-subtracted points were then plotted, and a smooth curve was drawn which gave a good visual fit to the data. The maximum of this curve is reported as the resonance

energy. The full width at half-maximum (FWHM) is reported as the total width, which includes a contribution from finite target thickness. The target thicknesses in all cases are less than 10 keV.

This technique was used by the present authors to analyze a large number of resonances in an earlier survey of isobaric-analog states by the  $(p,n)$  reaction.<sup>8</sup> There was reasonable agreement between energies and total widths determined in that survey and those observed in other  $(p,n)$  experiments. The major difficulty in analyzing data of this kind is the choice of a suitable background subtraction. For this reason, the results obtained using the graphical technique described above are essentially as reliable as those obtained using a computer program, which was originally written to examine the details of resonance shapes. When this program was used to fit the data to a background plus a single Breit-Wigner resonance, the results were in good agreement with those obtained by the graphical method. The errors quoted on the total widths in the present  $(p,n)$  work include uncertainties in the background subtraction, in addition to the estimated errors in drawing the best fit to the background-subtracted data.

In general, the  $(p,n)$  work served to identify the isobaric-analog resonances. Only those resonances showing appreciable strength in elastic scattering were analyzed using the single-level formula (Eq. 3.1). In the cases where the anomalies in elastic scattering were weak, resonances in the  $(p,n)$  excitation curves served as strong corroborative evidence for their identification as analog states.

Identification of corresponding states in the  $pC$  and

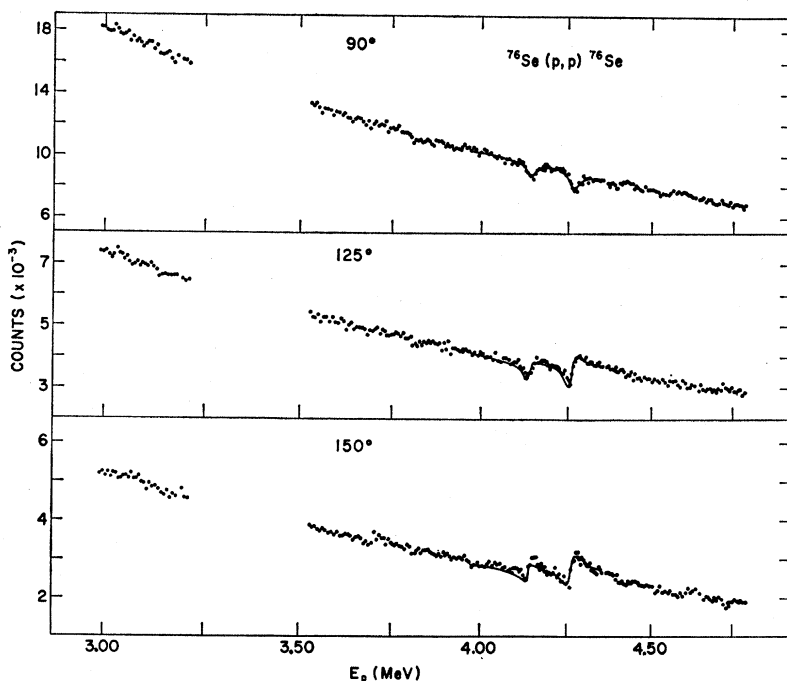


FIG. 2. Excitation curves for elastic scattering on  $^{76}\text{Se}$ . The solid curves represent fits to the data as described in the text.

$nC$  systems was facilitated by a semiempirical formula<sup>10</sup> for the Coulomb energy difference  $\Delta E_c$  between two nuclear states, defined as the energy required to replace a neutron by a proton in a given nuclear state, apart from the  $n$ - $p$  mass difference. The estimate of  $\Delta E_c$ , which is generally accurate to about 100 keV, together with the  $l$  value of the resonance, is usually sufficient to make an unambiguous identification. A further aid in identification is the proportionality between the reduced widths  $\gamma_p^2$  and  $\gamma_n^2$  [Eq. (1.1)]. This means that analogs of states with large stripping cross sections tend to show up strongly in elastic proton scattering.

The resonance parameters obtained in the present work are given in Table I, together with the level positions and  $l$  values obtained in the  $(d,p)$  study.<sup>6</sup> Once corresponding states have been identified, the excitation energies in the  $nC$  system were computed by arbitrarily assigning to the first analog state observed the excitation energy of the corresponding state observed in the  $(d,p)$  work.

The remainder of this section is devoted to a detailed examination of the resonances observed in the four nuclei studied.

#### $^{76}\text{Se}$

The  $(p,p)$  excitation curve for  $^{76}\text{Se}$  is shown in Fig. 2. Since the  $(p,n)$  threshold for  $^{76}\text{Se}$  is 5.4 MeV,<sup>11</sup> elastic proton scattering provides the simplest way to study the isobaric analogs of low-lying states in  $^{77}\text{Se}$ . The best fit to the strong  $l=0$  doublet at  $E_p=4.146$  and  $4.272$  MeV

is superimposed on the data points. The assignment of  $l$  values is easily made by noting that resonant structure appears at all three angles studied. These resonances are identified as the isobaric analogs of the two strong  $l_n=0$  states seen in the  $(d,p)$  work of Lin at excitations of 0.97 and 1.15 MeV in the residual nucleus.

With this identification, there is a 60-keV discrepancy between the energy separation of the two states in  $(p,p)$  elastic scattering and the value obtained from the  $(d,p)$  work. This degree of agreement is typical for most of the resonances observed in the present work. It should be pointed out that any interference effects between these two  $0^+$  resonances have been neglected. This should not affect the resonance parameters seriously, since the experimental excitation curves at three angles are quite well reproduced by the theoretical formula. (See Fig. 2.)

#### $^{78}\text{Se}$

The  $(p,n)$  excitation curve for  $^{78}\text{Se}$  is shown in Fig. 3. Six isobaric-analog resonances can be identified above the  $(p,n)$  threshold. All but two of these correspond to states formed by  $l=2$  neutrons in the  $(d,p)$  reaction. Penetrability effects make it easier to observe  $l=2$  resonances in the  $(p,n)$  reaction. The availability of many final states makes the decay of the analog resonances via  $l=0$  neutrons possible, whereas in the case of elastic scattering,  $l$  is restricted to 2 in both the entrance and exit channels.

The  $(p,p)$  excitation curve for  $^{78}\text{Se}$  is shown in Fig. 4, together with the best fits to the resonances analyzed. Measurement of a preliminary excitation curve at an angle of  $150^\circ$  over the energy range 3.5–5.2 MeV showed no appreciable structure for proton energies below 4.5

<sup>10</sup> D. D. Long, P. Richard, C. F. Moore, and J. D. Fox, Phys. Rev. **149**, 906 (1966).

<sup>11</sup> J. H. E. Mattauch, W. Thiele, and A. H. Wapstra, Nucl. Phys. **67**, 1 (1964).

MeV. Therefore only the region from 4.5 to 5.1 MeV was studied in detail. A strong  $s$ -wave resonance is observed at  $E_p=4.694$  MeV. This is identified as the analog of the strong  $l_n=0$  state observed at 1.16 MeV in the  $(d,p)$  experiment. With this identification, analogs of an  $l_n=2$  state at 1.25 MeV and an  $l_n=0$  state at 1.49 MeV are observed at proton energies of 4.808 and 5.809 MeV, respectively. The largest discrepancy in energy separation is 60 keV. Resonance energies for the three resonances observed in both elastic scattering and the  $(p,n)$  reaction are in good agreement; the total widths are in fair agreement.

### $^{80}\text{Se}$

Three low-lying isobaric-analog resonances in the reaction  $^{80}\text{Se}(p,n)$  have been studied previously in this laboratory.<sup>8</sup> In the present work the excitation curve has been extended to proton energies of 5.1 MeV. The complete  $(p,n)$  excitation curve is shown in Fig. 5.

The  $(p,p)$  excitation curve for  $^{80}\text{Se}$  is shown in Fig. 6. In this nucleus the analog of the ground state of  $^{81}\text{Se}$  is weakly excited at an incident proton energy of 3.817 MeV, and our  $l$ -value assignment of 1 is in agreement with the known spin<sup>12</sup> of  $\frac{1}{2}^-$  for the ground state of  $^{81}\text{Se}$ . There is also a strongly excited triplet of states at a proton energy of about 5 MeV. These resonances have been assigned  $l$  values of 2, 0, and 2 by noting that the first and third do not show any interference pattern at  $125^\circ$ . The largest energy shift relative to the levels observed in the  $(d,p)$  experiment is 100 keV; this is the largest shift observed in the present work.

The agreement between the  $(p,p)$  and  $(p,n)$  data is very good for  $^{80}\text{Se}$ , with the exception of the total width of the strong  $s$ -wave resonance at  $E_p=4.982$  MeV, which appears to be somewhat larger in the  $(p,n)$  reaction. This broadening of strong  $s$ -wave resonances in the  $(p,n)$  reaction relative to elastic proton scattering occurs also in  $^{82}\text{Se}$  in the present work (see below) and in a similar study<sup>8,13</sup> of  $^{76}\text{Ge}$ .

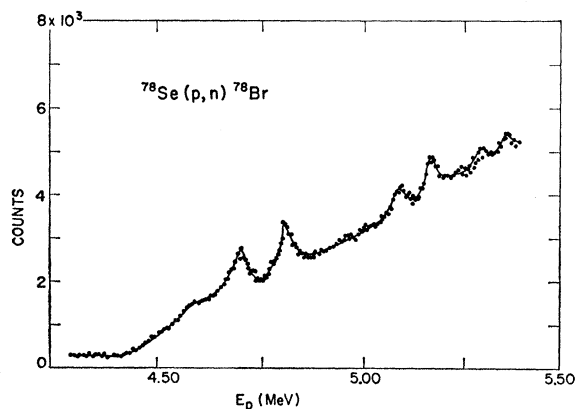


FIG. 3. Neutron excitation curves for the  $^{78}\text{Se}(p,n)^{78}\text{Br}$  reaction. The solid curve is merely to guide the eye.

<sup>12</sup> Nucl. Data B1, 4-87 (1966).

<sup>13</sup> G. E. Mitchell, D. P. Balamuth, G. P. Couchell, and R. N. Horoshko, Bull. Am. Phys. Soc. 12, 511 (1967).

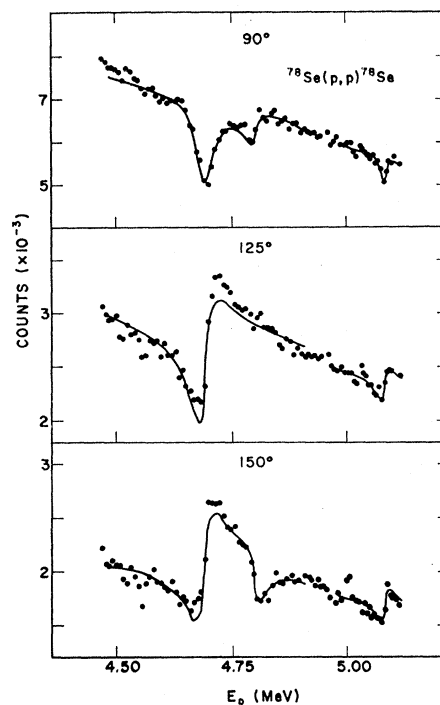


FIG. 4. Excitation curves for elastic scattering on  $^{78}\text{Se}$ . The solid curves represent fits to the data.

### $^{82}\text{Se}$

The excitation curve for  $^{82}\text{Se}(p,n)^{82}\text{Br}$  is shown in Fig. 7. The ground state of  $^{83}\text{Se}$  is known to have a spin<sup>14</sup> of  $\frac{9}{2}^+$ . Since  $l=4$  protons are required to form this state, one would not expect to observe this state in the present experiment. The first resonance in the  $(p,n)$  excitation curve is identified as the isobaric analog of the 0.36-MeV state observed in the  $(d,p)$  work. The strong doublet at  $E_p=5.148$  and 5.190 MeV is almost certainly the isobaric analog of the strongly excited state(s) occurring in the  $(d,p)$  work at an excitation energy of 0.59 MeV in

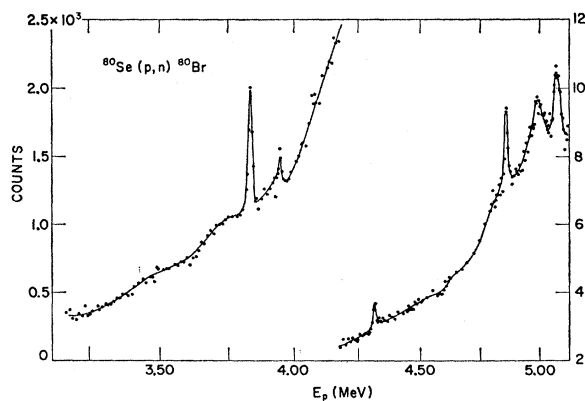


FIG. 5. Neutron excitation curve for  $^{80}\text{Se}(p,n)^{80}\text{Br}$ . Left-hand ordinate scale applies to the lower-energy portion of the data; the counts for the higher-energy part of the data are read from the right-hand scale. The solid line is to guide the eye.

<sup>14</sup> Nucl. Data B1, 4-129 (1966).

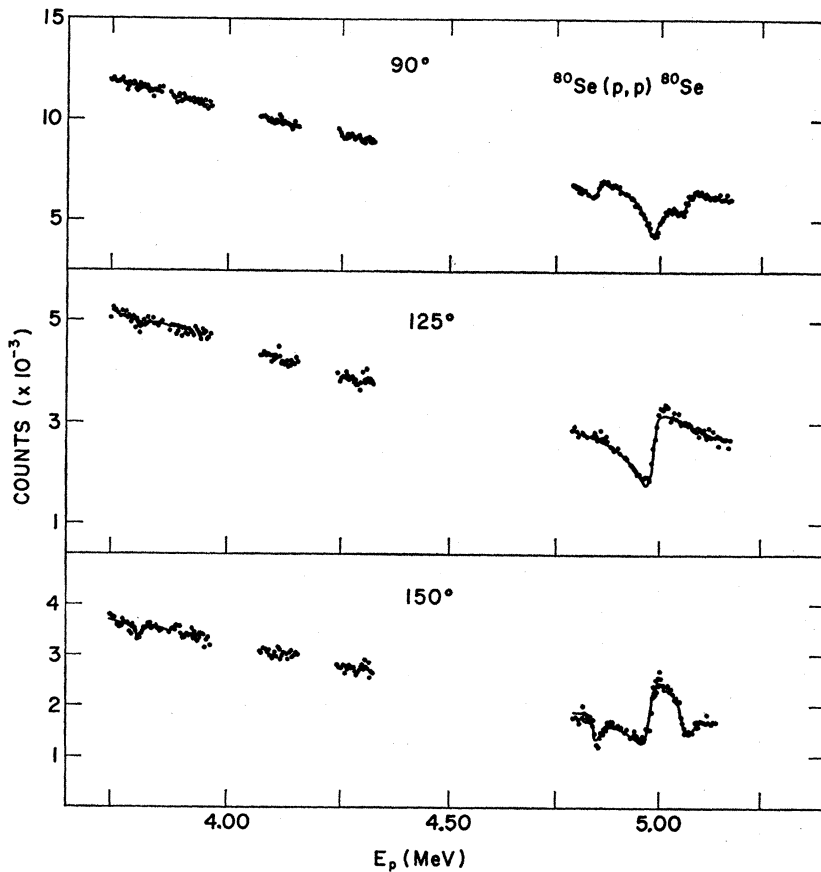


FIG. 6. Excitation curves for elastic scattering on  $^{80}\text{Se}$ . The solid curves represent fits to the data.

$^{83}\text{Se}$ , which is reported as a single state with  $l_n=2$ . Further evidence for this can be obtained from the  $^{82}\text{Se}(p,p)^{82}\text{Se}$  excitation curve, which is shown in Fig. 8. The anomaly at  $E_p \sim 5.15$  MeV shows a strong interference pattern at all angles, indicating that the resonance has a strong  $l=0$  component. The anomaly could not be fit consistently at all angles with single  $l=0$  resonance; the fit shown was made using an  $l=0, 2$  doublet. In the analysis the data at  $125^\circ$  were fitted first, giving parameters for the  $l=0$  state; the data at  $90^\circ$  and  $150^\circ$  were then fitted assuming two states. Again the agreement between the  $(p,n)$  work and the proton elastic scattering is quite good except for the apparent broadening of the strong  $s$ -wave resonance.

#### 4. COULOMB ENERGY DIFFERENCES

The availability of the high-resolution  $(d,p)$  studies makes possible determination of Coulomb energy differences for the four analog pairs ( $^{77}\text{Se}, ^{77}\text{Br}$ ), ( $^{79}\text{Se}, ^{79}\text{Br}$ ), ( $^{81}\text{Se}, ^{81}\text{Br}$ ), and ( $^{83}\text{Se}, ^{83}\text{Br}$ ). The Coulomb energy difference  $\Delta E_c$  can be extracted from the present data using the relation

$$\Delta E_c = [M_t / (M_t + M_p)] E_R + B_n - E_{\text{ex}}, \quad (4.1)$$

where  $E_R$  is the laboratory energy of the proton at resonance;  $M_t$  and  $M_p$  are the masses of the target and

proton, respectively;  $B_n$  is the neutron separation energy from the nucleus  $nC$ , where  $C$  is the target; and  $E_{\text{ex}}$  is the excitation of the corresponding state in the nucleus  $nC$ . In the present work  $B_n$  was obtained from the mass tables of Mattauch *et al.*<sup>11</sup>

Since a strong  $s$ -wave resonance is observed in all of the isotopes studied, the Coulomb energy difference  $\Delta E_c$  was calculated for these states. The results are presented in Table II, together with the value of  $\Delta E_c$ .

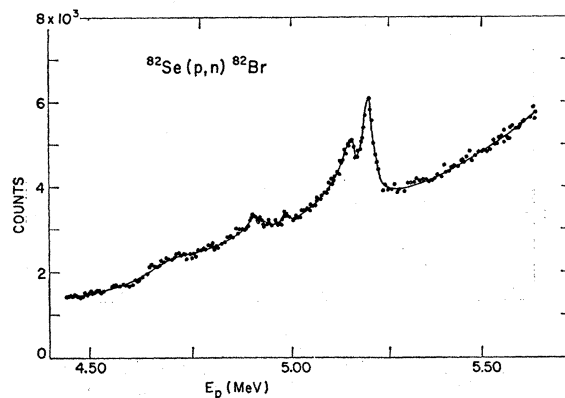


FIG. 7. Neutron excitation curve for  $^{82}\text{Se}(p,n)^{82}\text{Br}$ . The solid curve is to guide the eye.

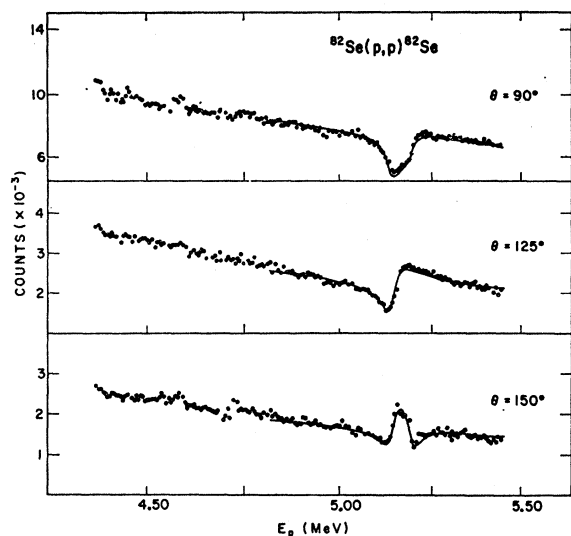


FIG. 8. Excitation curves for elastic scattering on  $^{82}\text{Se}$ . The solid curves represent fits to the data.

predicted by a semiempirical formula

$$\Delta E_c = -1.032 + 1.448Z/A^{1/3}. \quad (4.2)$$

This formula was obtained by Long *et al.*,<sup>10</sup> who performed a least-squares fit of available Coulomb energy differences to a form linear in  $Z/A^{1/3}$ . The observed Coulomb displacement energies are seen to be given fairly well by the semiempirical formula with the exception of ( $^{82}\text{Se}$ ,  $^{82}\text{Br}$ ), which departs from the expected systematic decrease of  $\Delta E_c$  with increasing neutron excess. It is interesting to note that the ( $d, p$ ) studies of the selenium isotopes indicate that the  $p_{1/2}$  shell is mostly empty in  $^{76}\text{Se}$ ,  $^{78}\text{Se}$ , and  $^{80}\text{Se}$ , since a strongly excited  $\frac{1}{2}^-$  state is observed with a large spectroscopic factor at low excitation energy. On the other hand, in  $^{82}\text{Se}$  a  $\frac{1}{2}^-$  state is observed very weakly. Lin points out that this is probably a consequence of the  $p_{1/2}$  shell being nearly full in  $^{82}\text{Se}$ . It is quite possible that the anomalous value of the Coulomb energy difference is connected with the different core configuration in  $^{82}\text{Se}$ .

## 5. SPECTROSCOPIC FACTORS

Spectroscopic factors have been calculated for all resonances observed in elastic scattering in the present work using the computer program ANSPEC,<sup>15</sup> written by Thompson and Adams. The program calculates the quantity

$$S_n = \frac{\gamma_n^2(a_c)}{\gamma_{nsp}^2(a_c)} = (2T_0 + 1) \left( \frac{\Gamma_{\lambda p}}{2P_p(a_c)} \right) \frac{1}{\gamma_{nsp}^2(a_c)}, \quad (5.1)$$

where  $\Gamma_{\lambda p}$  is the partial width of the resonance for proton elastic scattering,  $T_0$  is the isospin of the target,  $P_p$  is the penetrability, and  $\gamma_{nsp}^2$  is the neutron single-

<sup>15</sup> W. J. Thompson and J. L. Adams, ANSPEC, Florida State University Technical Report No. 10, 1967 (unpublished).

TABLE II. Coulomb displacement energies for the strongest  $s$ -wave resonance observed in each isotope. The experimental  $\Delta E_c$  is the displacement energy determined in the present work, while the calculated  $\Delta E_c$  is the result predicted from Eq. (4.2).

	Experimental $\Delta E_c$ (MeV)	Calculated $\Delta E_c$ (MeV)
$^{77}\text{Se}-^{77}\text{Br}$	$10.48 \pm 0.02$	10.54
$^{78}\text{Se}-^{78}\text{Br}$	$10.45 \pm 0.02$	10.44
$^{81}\text{Se}-^{81}\text{Br}$	$10.39 \pm 0.02$	10.35
$^{82}\text{Se}-^{82}\text{Br}$	$10.47 \pm 0.05$	10.25

particle reduced width, given by

$$\gamma_{nsp}^2(a_c) = (\hbar^2/2ma_c)u_n^2(a_c). \quad (5.2)$$

The radial wave function  $u_n(r)$  is the solution to the bound-state problem of a neutron in a real potential  $V_n(r|J)$ , subject to the boundary conditions

$$u_n(0) = 0, \quad u_n(r) \rightarrow 0 \quad \text{as } r \rightarrow \infty. \quad (5.3)$$

The form used for  $V_n(r|J)$  is a Saxon-Woods potential with radius  $= 1.25A^{1/3}$  F. and diffuseness  $= 0.65$  F. The well depth is determined by fixing the neutron binding energy  $\epsilon = \Delta E_c - E_\lambda$ , where  $\Delta E_c$  is the measured Coulomb energy difference for the state in question, and  $E_\lambda$  is the resonance energy in the center-of-mass system. The well depth is then varied until the conditions (5.3) are satisfied.

Following the suggestion of Robson,<sup>16</sup> the matching radius  $a_c$  in (5.1) is taken as  $R_c^- = 1.05A^{1/3} + 1.5$  F. With this choice of  $a_c$ , which is close to the outer charge radius of the target, the penetrability  $P_p(a_c)$  can not be accurately represented by the usual Coulomb penetrability  $P_c = kr/(F_l^2 + G_l^2)$ , where  $F_l$  and  $G_l$  are the regular and irregular Coulomb functions. To include the effect of nuclear forces approximately, the penetrability calculation is made using wave functions derived from an optical-model potential. A set of optical-model parameters were chosen to describe the nonresonant scattering of protons from selenium at  $E_p \sim 5$  MeV. These were largely extrapolated from those of Perey,<sup>17</sup> except for the surface absorption strength  $W$ , which was set equal to 5 MeV following the suggestion of Thompson.<sup>18</sup> The potential used was

$$V_{\text{optical}} = -Uf(r) - iWg(r) - U_{s0}(2\mathbf{l} \cdot \mathbf{s})h(r) + V_c(r), \quad (5.4)$$

TABLE III. Optical-model potential parameters used in the calculation of spectroscopic factors  $S_n$ , as described in the text.

Nucleus	$U$ (MeV)	$W$ (MeV)	$U_{s0}$ (MeV)	$R$ (F)	$a$ (F)	$a'$ (F)
$^{76}\text{Se}$	57.0	5	7.5	$1.25A^{1/3}$	0.65	0.47
$^{78}\text{Se}$	57.4	5	7.5	$1.25A^{1/3}$	0.65	0.47
$^{80}\text{Se}$	57.9	5	7.5	$1.25A^{1/3}$	0.65	0.47
$^{82}\text{Se}$	58.2	5	7.5	$1.25A^{1/3}$	0.65	0.47

<sup>16</sup> D. Robson, in Ref. 4, pp. 411-431.

<sup>17</sup> F. G. Perey, Phys. Rev. **131**, 745 (1963).

<sup>18</sup> W. J. Thompson (private communication).

TABLE IV. Spectroscopic factors for resonances observed in elastic scattering and comparison with  $(d,p)$  work (Ref. 6). The spin assignments are those of Ref. 6.

Nucleus	$E_{\text{c.m.}}$	$J^\pi$	$S_n$	$S_{dp}$ *
$^{76}\text{Se}$	4.092	$(\frac{1}{2})^+$	0.16	0.13
	4.216	$(\frac{3}{2})^+$	0.32	0.38
$^{78}\text{Se}$	4.635	$(\frac{1}{2})^+$	0.98	0.66
	4.747	$(\frac{3}{2})^+$	0.30	0.34
	5.025	$(\frac{5}{2})^+$	0.081	0.066
$^{80}\text{Se}$	3.770	$(\frac{1}{2})^-$	0.093	0.30
	4.787	$(\frac{3}{2})^+$	0.18	0.26
	4.920	$(\frac{5}{2})^+$	0.85	0.64
	4.998	$(\frac{7}{2})^+$	0.41	0.40
$^{82}\text{Se}$	5.086	$(\frac{1}{2})^+$	0.63	0.62
	5.127	$(\frac{3}{2})^+$	0.57	

\* Reference 1.

where

$$\begin{aligned}
 f(r) &= \{1 + \exp[(r-R)/a]\}^{-1}, \\
 g(r) &= 4 \exp[(r-R)/a'] \{1 + \exp[(r-R)/a']\}^{-2}, \\
 h(r) &= (ra)^{-1} \exp[(r-R)/a] \{1 + \exp[(r-R)/a]\}^{-2}, \\
 V_c(r) &= Z_p Z_T (e^2/2R) [3 - (r/R)^2], \quad r < R \\
 &= Z_p Z_T (e^2/r), \quad r > R.
 \end{aligned}$$

The optical-model parameters used in the present work are listed in Table III. The spectroscopic factors calculated in this way can be compared directly with spectroscopic factors  $S_{dp}$  obtained from stripping data.<sup>15,16</sup>

The spectroscopic factors calculated from the present experimental data using the above procedure are shown in Table IV, together with the spectroscopic factors obtained in the  $(d,p)$  study of Lin.<sup>6</sup> For ease of comparison, the spin assignments from the  $(d,p)$  experiment were used in calculating the spectroscopic factors  $S_n$ , although only  $(2J+1)\Gamma_{\lambda p}$  was determined from the elastic scattering data.

The spectroscopic factors determined in the present work are in reasonable agreement with those obtained in the  $(d,p)$  experiment.<sup>6</sup> However, it should be pointed out that one major difficulty in extracting quantitatively reliable spectroscopic factors is that the spectroscopic factors determined by the method outlined

TABLE V. Relative spectroscopic factors for two states with the indicated  $J^\pi$ , shown as a function of the real well depth  $U$  in the optical potential.

Nucleus	$J^\pi$	$U$ (MeV)	$S_2/S_1$
$^{76}\text{Se}$	$(\frac{1}{2})^+$	52.0	2.2
	$(\frac{3}{2})^+$	57.0	1.9
	$(\frac{5}{2})^+$	62.0	2.1
$^{78}\text{Se}$	$(\frac{1}{2})^+$	52.4	0.14
	$(\frac{3}{2})^+$	57.4	0.08
	$(\frac{5}{2})^+$	62.4	0.08
$^{80}\text{Se}$	$(\frac{3}{2})^+$	53.2	2.5
	$(\frac{5}{2})^+$	58.2	2.3
	$(\frac{7}{2})^+$	63.2	2.3

above are sensitive to the optical-model parameters used in describing the  $pC$  system. In the present study the spectroscopic factors for  $s$ -wave resonances seem to be the most strongly affected by variations in the optical potential.

Many of the above difficulties can be minimized by considering only *relative* spectroscopic factors in a given nucleus. If the same optical potential is used in calculating the penetrability  $P_p$ , the quantity  $S_\lambda/S_{\lambda'}$  for two resonances  $\lambda$  and  $\lambda'$  with the same  $l$  value should not be very sensitive to the optical-model parameters. There are three cases where this can be tested in the present work. Table V shows relative spectroscopic factors for three different nuclei calculated using a real well depth of  $U^{(0)}$ ,  $U^{(0)} + (5 \text{ MeV})$ , and  $U^{(0)} - (5 \text{ MeV})$ , where  $U^{(0)}$  is the value in Table III. Examination of Table V shows that the relative spectroscopic factors are not very sensitive to even substantial changes in the real well depth.

#### ACKNOWLEDGMENTS

The authors would like to thank Professor C. F. Moore and Dr. P. Richard for the computer program SNOW and Professor W. J. Thompson and Dr. J. L. Adams for the program ANSPEC. Valuable conversations with Professor Moore and Professor Thompson are also gratefully acknowledged. The assistance of W. Patton in both collecting the experimental data and in writing programs for processing the data is particularly appreciated.